COHERENCE OF E-BEAM RADIATION SOURCES AND FELS – A THEORETICAL OVERVIEW

Avi Gover, Egor Dyunin, Tel-Aviv University, Ramat Aviv, Israel.

GENERAL FORMULATION FOR RADIATION EMISSION FROM MICROSCOPIC CHARGES

This publication is mostly tutorial. It presents a general time-frequency modal-expansion linear formulation for radiation excitation from charges. This, however, can be employed to analyze front-line FEL research problems. Starting from description of synchrotron undulator radiation, the model is extended to describe the coherence characteristics of stimulated emission devices (FEL amplifiers and oscillators), and then further extended to the SASE regime. It is then employed to point out directions for development of coherent X-UV FEL sources.

The starting point of our formulation is the general Maxwell Equations driven by particulate point charge sources (the source dimension is smaller than the emission wavelength):

$$\nabla \times \mathbf{E} = -\mu \frac{\partial \mathbf{H}}{\partial t} - \mu_0 \frac{\partial \mathbf{M}}{\partial t}$$
$$\nabla \times \mathbf{H} = \varepsilon \frac{\partial \mathbf{E}}{\partial t} + \mathbf{J} + \frac{\partial \mathbf{P}}{\partial t} \qquad (1)$$

where in general the point sources may be free electrons, atomic electric dipoles or atomic magnetic dipoles and spins [1]:

$$\mathbf{J} = \sum_{j=1}^{N} -e\mathbf{v}_j \delta(\mathbf{r} - \mathbf{r}_j(t))$$

$$\mathbf{P} = \sum_{j=1}^{N} \mathbf{p}_j \delta(\mathbf{r} - \mathbf{r}_j(t)) \qquad (2)$$

$$\mathbf{M} = \sum_{j=1}^{N} \boldsymbol{\mu}_j \delta(\mathbf{r} - \mathbf{r}_j(t))$$

In this article we focus on free electrons.

Maxwell Equations can be exceedingly simplified in the frequency domain. In the frequency domain it is possible in many structures to expand the radiation field in terms of a complete set of eigenmodes { $\tilde{\mathbf{E}}_q$ }:

$$\tilde{\mathbf{E}}(\mathbf{r}, \omega) = \sum_q C_q(z, \omega) \tilde{\mathbf{E}}_q(\mathbf{r}) \qquad (3)$$

This certainly can be done in a waveguide, but also in free-space, where one can use a discrete set of modes like Hermit-Gaussian modes, commonly used in laser physics, or continuous modes – like plane waves. In this latter case the summation of q degenerates into integration over transverse wave numbers.

After modal expansion it is possible to simplify Maxwell's set of 3-D differential equations into a simple infinite set of first order ordinary differential equations for the complex amplitudes $C_q(z, \omega)$ [2,3]. These can be solved for each mode at steady state, if the initial condition $C_q^{in}(\omega)$ (the complex amplitudes at the entrance to the interaction region) is given (see Fig.1). The formal solution for the increment of the complex amplitudes in the case of *free electron* microscopic charges is:

$$C_q^{out}(\omega) - C_q^{in}(\omega) = \sum_{j=1}^{N} \Delta C_{qj} =$$
$$= -\frac{1}{4} \sum_{j=1}^{N} \left\{ -e \int_{-\infty}^{\infty} \mathbf{v}_j(t) \cdot \tilde{\mathbf{E}}_q^*(\mathbf{r}_j(t)) e^{i\omega t} dt \right\} \qquad (4)$$

For any charges in the interaction volume the output amplitudes C_q^{out} can be calculated. Thus the entire output radiation field can be calculated then by substituting $\{C_q^{out}\}$ back into the expansion series (3), or using it otherwise to calculate optical parameters.
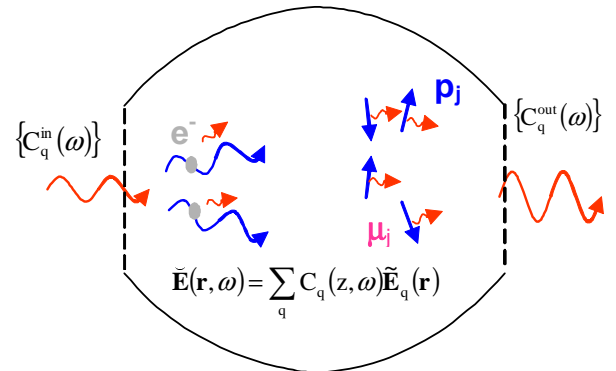

Fig.1: Excitation of radiation modes by particulate charges (Frequency Domain).

This suggests the following picture for modal excitation: the field amplitude increment of each mode is composed of the sum of contributions from the individual electrons, which correspond to the "wavepackets" emitted by the individual electrons. To calculate the increment to the radiation mode amplitude, one must solve a contour integral along the trajectory of each electron and sum up the wavepacket contributions.

In principle, the trajectories can be expanded in series in terms of the field amplitudes C_q. To zero order, the trajectories of the electrons are not modified by the radiation field and we know them explicitly. In this case the contour integrals can be performed straightforwardly. If all the electrons have the same trajectories (a narrow beam), then their wavepacket amplitudes are identical, except for a "start oscillation" or "entrance time" phase factor [3]:

$$C_q^{out}(\omega) = C_q^{in}(\omega) + \Delta C_{qe}^{(0)}(\omega) \sum_{j=1}^{N} e^{i\omega t_{oj}} + \sum_{j=1}^{N} \Delta C_{qj}^{st} \quad (5)$$

The contribution of the electrons to the total field depends to *zero order* in the fields on the phase relation between the wavepackets. These contributions (second term in (5)) give rise to the *spontaneous* or *superradiant* emission of the electron beam [3]. At higher order of expansion in terms of the fields, the modification of the electron trajectories by the fields, gives rise to *stimulated emission* or *stimulated absorption*, represented by the last term of (5).

Once one calculated the mode amplitudes (5) it is possible to substitute them in (3) to find the total field. Alternatively, one can use them to calculate optical parameters as radiation mode power or spectral energy (both are quadratic forms of C_q):

$$P_q = \left| C_q^{out}(\omega) \right|^2 \quad \text{or} \quad \frac{dW_q}{d\omega} = \frac{2}{\pi} \left| C_q^{out}(\omega) \right|^2 \quad (6)$$

Several physical situations can be distinguished, corresponding to the manner the amplitudes in (5) combine in the complex $C_q(\omega)$ plane to produce the total radiation field. These are shown graphically in Fig.2 [3]. Let us now neglect the stimulated emission terms, and assume no input field $C_q^{in}(\omega) = 0$. When one absolute value square the second term in (5) and then average over the electron phases j, one can distinguish two cases, corresponding to two different emission processes:

(1) The electron entrance times are random (Fig.2a). In this case only the non-mixed terms in the square of the sum do not average down to zero ($\left\langle \sum_{j=1;\, j\neq i}^{N} e^{i\omega t_{oj}} \cdot e^{i\omega t_{oi}} \right\rangle_j = 0$), consequently the spectral energy is proportional to the number of particles N. This process is referred to as *spontaneous emission* or *shot noise emission*, and radiation spectral energy (6) is proportional to:

$$\left\langle \left| \sum_{j=1}^{N} e^{i\omega t_{oj}} \right|^2 \right\rangle_j = N \quad (7)$$

(2) The electron entrance times are correlated (Fig.2b): either they enter in a bunch of duration shorter than the radiation period, or periodically at the radiation frequency. In these cases the wavepackets emitted by the individual electrons interfere in phase with each other, and the spectral power is proportional to N^2:

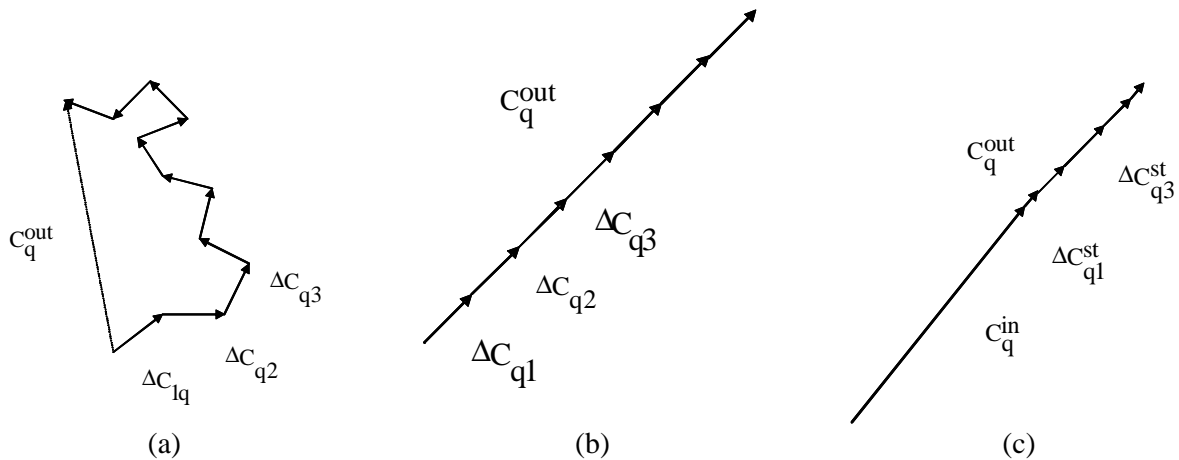(a)   (b)   (c)

Fig.2: Superposition of mode wavepacket amplitudes of electrons C_{qj} in the complex plane: a) spontaneous emission, b) superradiant emission, c) stimulated emission.

FEL Prize and New Lasing

$$\left\langle \left| \sum_{j=1}^{N} e^{i\omega t_{oj}} \right|^2 \right\rangle_j = N^2 \qquad (8)$$

We term this emission process "superradiance", following Dicke [4], who analyzed this case for an ensemble of molecules having electric or magnetic dipoles, employing a full quantum formulation (note though that the superradiance effect is classical even in Dicke's problem [1]). Superradiant emission is also termed *coherent emission*, as in CSR [5].

(3) When the mode field amplitudes at entrance do not equal to zero ($C_q^{in} \neq 0$) (Fig.2c), the electron trajectories may be modified by the presence of the radiation field, and the integral (4) will result in, beyond the zero order expansion approximation, a field-dependent radiation term (third term in (5)). This is the *stimulated Emission* term. In first order expansion in the fields (linear regime), neglecting inter-mode scattering, and this term is proportional to the mode field amplitude:

$$\sum_{j=1}^{N} \Delta C_{qj}^{st} \propto C_q$$

and therefore produces radiation wavepackets in phase with the incoming wave of amplitude C_q^{in}, and the total radiation is coherent.

UNDULATOR RADIATION OF A SINGLE ELECTRON

The formalism and classification described in the previous section can be applied to any kind of radiation mechanism: undulator, synchrotron, Smith-Purcell etc. [3, 6]. We now concentrate on the case of radiative emission in an undulator. Expressing the radiation field both in frequency domain and time domain, helps to understand the coherence characteristics of undulator radiation and FEL devices. We therefore will employ on occasions inverse Fourier transform on the radiation expressions which are generally derived in this formulation in the frequency domain.

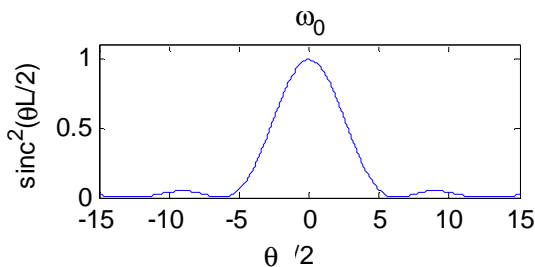The frequency domain amplitude of a wavepacket

Fig.3 The spectral emission curve of undulator radiation of single electron emission.

emitted into transverse mode q by a single electron traversing through an undulator is calculated from (4):

$$C_q^{out}(\omega) = -\frac{1}{4}\left\{ -e \int_{-\infty}^{\infty} \mathbf{v}_j(t) \cdot \tilde{\mathbf{E}}_q^{\,*}(\mathbf{r}_j(t)) e^{i\omega t}\, dt \right\} \qquad (9)$$

$$\mathbf{v}_j(t) = \mathrm{Re}\left\{ \tilde{\mathbf{v}}_w e^{-ik_w z_j(t)} \right\} + v_z \hat{\mathbf{e}}_{\mathbf{z}}$$

The result is:

$$C_{qj}^{out}(\omega) = e \frac{\mathbf{v}_w \cdot \mathbf{E}_q^*(\mathbf{r}_{\perp 0})}{8v_z} L \,\mathrm{sinc}(\theta(\omega)L/2)\, e^{i\theta(\omega)L/2}\, e^{i\omega t_{0j}} \qquad (10)$$

where $\theta(\omega)L \equiv \left(\dfrac{\omega}{v_z} - k_z(\omega) - k_w \right)L = (\omega - \omega_0)t_{sl}$ is the

detuning parameter); $t_{sl} = \dfrac{2\pi}{\Delta\omega} = \dfrac{L}{v_z} - \dfrac{L}{v_g}$ is the slippage

time, and ω_0, the synchronism frequency, is defined from $\theta(\omega_0) = 0$. Substituted in (6), this is a resonant emission linewidth function, centered on the synchronism frequency, and having a frequency bandwidth equal to the inverse of the slippage time (Fig.3):

Note that the amplitudes (10) of the wavepackets C_{qj}^{out} of different electrons differ only by a phase factor (as in (5))!

One can describe the wavepacket field in the time domain by performing an inverse Fourier transform over the complex amplitude function (10):

$$\mathbf{E}(\mathbf{r},t) = \mathbf{F}^{-1}\left\{ C_q(z,\omega)\mathbf{E}_q(\mathbf{r}_\perp)e^{ik_z(\omega)z} \right\} =$$

$$= \sum_{i=1}^{2} A_i \mathbf{E}_q(\mathbf{r}_\perp)\cos(k_z(\omega_i)z - \omega_i t)\,\mathrm{rect}\left[\frac{t - z/v_z + t_{sl_i}/2}{|t_{sl_i}|} \right] \qquad (11)$$

In the time domain, the wavepacket is composed of two simple truncated sinusoidal waveforms (Fig.4). The *high frequency* radiation wavepacket of slippage time duration t_{sl1} arrives first after a retardation time L/v_{g1}; then the electron arrives after time L/v_z and at the end the *low frequency* wavepacket, corresponding to backward emission in the electron rest-frame, arrives with a radiation (back-slippage) time L/v_{g2} [7]. Here v_{g1}, v_{g2} are the group velocities of the waves propagation in a waveguide enclosure [7]. In free space $v_{g1} = c$, $v_{g2} = -c$ and the low frequency wavepacket is actually emitted backward also in the lab frame. In any case this low frequency wavepacket is not important for the present discussion and will be neglected in the subsequent discussion.
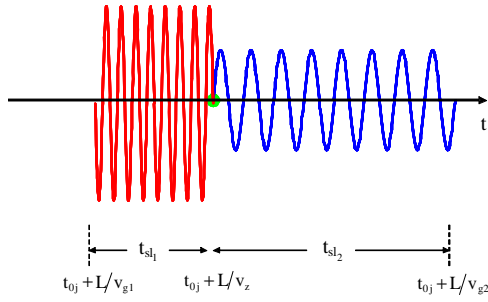
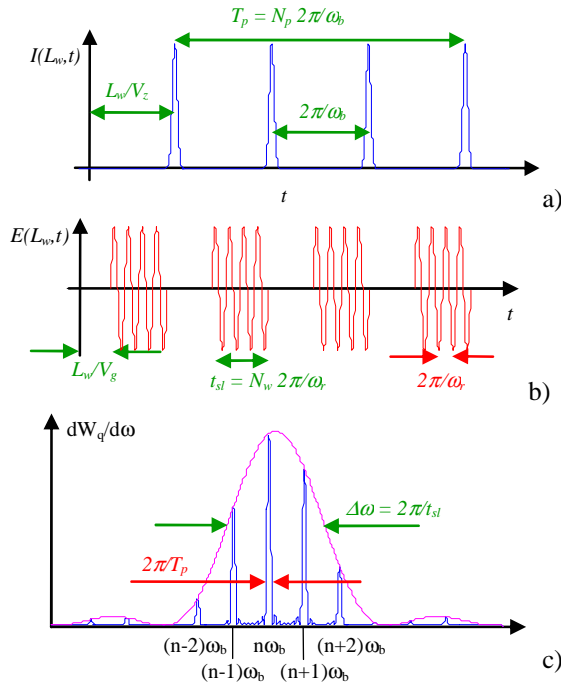Fig.4: Time domain waveform of a single electron emission wavepacket.

Fig.5: Superradiant (coherent) radiative emission from a macropulse train of e-beam bunches:
  a) current waveform; b) time domain picture of the train of phase coherent radiation wavepackets;
  c) spectral power of the radiation field waveform (b).

UNDULATOR RADIATIVE EMISSION OF A BUNCH OF ELECTRONS

If we consider now emission from a bunch of N electrons, its resultant radiative emission field will be composed of a superposition of wavepackets like the one in Fig.4 [3]. In the frequency domain the emission amplitude from all electrons (10) is the same except for a phase factor. Therefore the spectral emission curve is the same function as of a single electron (Fig.3). It is multiplied by N in the case of spontaneous emission (when t_{0j} is random - see Eq.7) or by N^2 in the case of superradiant emission (when $|t_{0j}-t_0| < 2\pi/\omega$ - see Eq.8).

EMISSION OF A PERIODIC TRAIN OF ELECTRON BUNCHES

Examine now superradianat radiative emission from a train of electron bunches, for example a macro pulse of an RF accelerator (Fig.5a).

The periodic bunches radiate independently of each other. The resultant radiation waveform (Fig.5b) is a temporal periodic sequence of the single bunch wavepackets of Fig.4 (only the high frequency wavepackets are considered). The duration of the electron beam macropulse is $T_p = N_p*2\pi/\omega_b$: the number of electron bunches N_p times the bunching period. The duration of the wavepacket is $t_{sl} = N_w*2\pi/\omega_r$: the number of wiggles N_w times the optical radiation period. The Fourier transform of the wave is dominated by these two time constants. Fig.5c displays the spectral power of this waveform (frequency domain) for the common case where $t_{sl} << 2\pi/\omega_b$. In this case there is no overlap between the wavepackets, and consequently there are several harmonics under the emission curve.

In the frequency domain, the macropulse spectral emission curve is the product of the single electron emission curve (the absolute value square of (10) – Fig.3) and the macropulse "form factor" [3]:

$$M_M(\omega) = \left[\frac{\sin(N_P \pi\omega / \omega_b)}{N_P \sin(\pi\omega / \omega_b)} \right]^2 \qquad (12)$$

The emission is wide band ($2\pi/t_{sl}$), but if one can filter out one harmonic, or if $\omega_b > \Delta\omega_{sl}$, it will have a narrow linewidth corresponding to the macropulse duration (under the condition of *stability* of the bunching frequency during the entire macropulse duration). This observation will be important also for the later discussion on the case of FEL oscillator and SASE.

A nice verification of this concept was demonstrated by the MIT research group [8] who measured superradiant Smith-Purcell coherent emission using an RF Linac beam. Carefully filtering out the radiation emission at the 14th harmonic of the microbunch repetition rate within the macropulse by *heterodyne* detection *techniques*, they measured the exceedingly narrow linewidth of the total waveform of the macropoulse radiation. It was indeed $2\pi/T_p$, corresponding to the duration T_p of the e-beam macropulse.

If the electron bunch has a finite duration t_b, then the expression for radiation spectral energy includes also a "bunch–form factor"

$$|M_B(\omega)|^2 = \left| \frac{1}{Q} \int_{-\pi/\omega_b}^{\pi/\omega_b} I(t) e^{i\omega t} dt \right|^2 \qquad (13)$$

(which is equal to unity as long as $t_b << 2\pi/\omega$).
This, in practice, limits the harmonic number n_H, that can have appreciable amplitude out of the infinite numbers of harmonics that the macropulse form factor (12) admits, to

$$n_H << 2\pi/\omega t_b \qquad (14)$$

If the waveform of the electron-beam current does not contain high harmonics (e.g. it is sinusoidally modulated) then there will be no harmonics under the spectral energy curve in Fig.5b except the fundamental ($n_H=1$), and its amplitude will be appreciable only within the bandwidth of the single electron emission spectrum ($\omega-\omega_b) < \Delta\omega = 2\pi/t_{sl}$. The narrow linewidth ($\delta\omega \sim 2\pi/T_p$) radiation of the prebunched FEL follows the detuning curve of Fig.3 as demonstrated experimentally in [22].

Single harmonic radiative emission can take place also at high harmonic n_H of the bunching frequency ω_b. This will happen (under the condition (14)) if the spacing between the harmonics exceeds the emission bandwidth:

$$\omega_b > \Delta\omega_{sl} = 2\pi/t_{sl}$$
$$\text{or} \qquad n_H < 2\pi/\omega_0 t_{sl} \cong N_w \qquad (15)$$

In this case, the wavepackets train of Fig.5b merges into an harmonic wave of the macropulse duration T_p.

FEL AMPLIFIER

Our main interest is in stimulated emission. Many of the spectral features of superradiant emission discussed above apply quite closely also to stimulated emission in an amplifier configuration. The derivation of the increments ΔC_q^{st} in the wavepacket amplitudes (third term in Eq.5) in the amplifier case is more involved, since it requires the calculation of the modification of the electron trajectories by the input radiation field. When this is done, it is found that also in this case the electron beam is bunched. The classical stimulated emission from an electron beam, always involves electron beam density
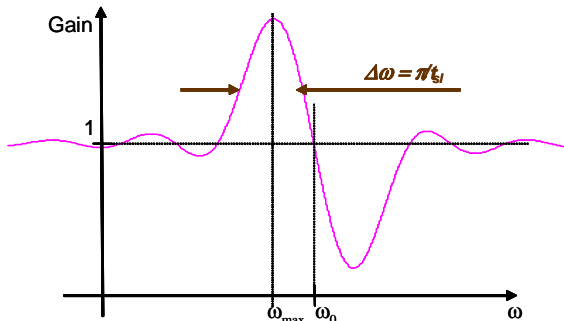
bunching. Contrary to superradiance the bunching is not set *ab-initio*, before entrance into the interaction region, but it is created by the input radiation signal, at the signal frequency, in the first part of the wiggler.

As well known, in a CW (or long pulse) FEL amplifier the single mode (1-D) incremental power gain is given in the linear (small signal) small gain regime by (see Fig.6) [6, 16]:

$$\frac{\Delta P}{P} = \overline{Q}\,\frac{d}{d\overline{\theta}}\,\mathrm{sinc}^2\left(\overline{\theta}(\omega)/2\right) \qquad (16)$$

The frequency ω of the electron bunching and the consequent radiation is determined by the input radiation signal. Thus the bandwidth of emitted radiation is determined by the bandwidth of the input signal, and if it is monochromatic then the output radiation is temporally coherent (except for admixture of noise (spontaneous undulator radiation) power emitted in the wiggler. Note however that the gain curve (16) (Fig.6, which is the derivative of the spontaneous emission spectral curve Fig.3) is quite wide still – about one half the width of the spontaneous emission curve $\Delta\omega_{st} = \pi/t_{sl}$.
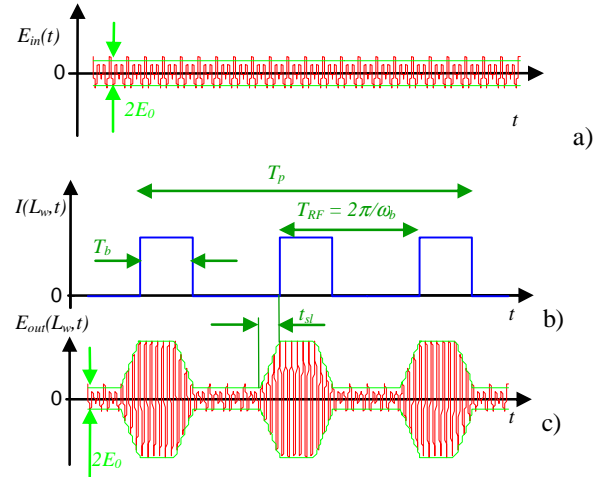

Fig.7: RF-Linac FEL Amplifier in the time domain.
a) multi-frquency coherent input signal
b) Electron beam macropulse current waveform
c) Amplified signal.

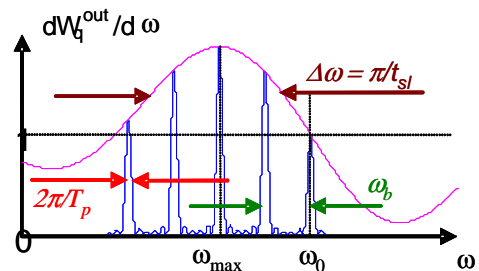

Fig.6: The FEL Linear regime small-gain curve.

Fig.8: Spectral power of the amplifier output radiation waveform of Fig.7c.

If the electron beam is not continuous, of course, its temporal wave-form will modify the spectrum of the amplifier radiation output. Let us consider an FEL amplifier fed by a train of electron beam pulses (microbunches) from a continuously operating RF-LINAC (see Fig.7b). The electron macropulse duration, micropulse duration and repetition period are typically $T_p = 10$ μs, $T_b \sim$ ps, $T_{RF} \sim$ ns respectively. The radiation signal period (say is the visible spectral region) $2\pi/\omega_0 \sim$ fs and the slippage time $N_w 2\pi/\omega_0 \sim 10 - 100$ fs, are both much shorter than the pulse duration T_b.

Fig.7 depicts this case in the time domain. For didactic reasons we assume that the input radiation (Fig.7a) is a *coherent* multi-frequency wide spectrum signal, wider than the gain bandwidth of the FEL ($\Delta\omega_{st} \sim \pi/t_{sl}$). The output signal (Fig.7c) is time gated by the waveform of the electron beam (Fig.7b) and also frequency filtered by the gain bandwidth of the FEL during the pulse duration.

The same case is displayed in the frquency domain in Fig.8. Only radiation frequencies within the gain bandwidth π/t_{sl} of the gain curve Fig.6 are amplified. Among the amplified frqeuncies only the ones which are harmonics of the bunching frequency ω_b, within a

frqeuncy deviation $\Delta\omega \sim 2\pi/T_p$ will contribute coherently to a Fourier transformation of the waveform in Fig.7c (carried out over the entire macropulse). Consequently the amplified signal spectrum will contain harmonics of ω_b, of linewidth $2\pi/T_p$.

RF – LINAC FEL OSCILLATOR

In laser physics it is customary to present an oscillator as an amplifier with feedback. In each round-trip a radiation wave-packet synchronous with an overlapping e-beam bunch gets amplified and is reflected back by mirrors into the entrance to the interaction region. It is assumed that the bunching frequency is commensurate with the round-trip frequency of the resonator: a new e-beam bunch arrives together with the radiation pulse, and the amplification process continues up to steady state saturation.

How does the saturation of an RF Linac FEL look in the time domain? Fig.9 displays the steady state waveform of the oscillator radiation in the time domain. It displays radiation pulses emitted synchronousely with the RF bunches, somewhat modified by the slippage effect (as in the amplifier case – compare to Fig.7c).

In the frequency domain (Fig.10a), the single path gain curve is the same as in the amplifier (Fig.8), and the RF frequency of the e-beam bunches is synchronized (by cavity length detuning) with the round-trip frequency of the radiation pulses – namely the longitudinal modes of the resonator. In addition, in the oscillator there is a gain threshold condition: $P_{out}/P_{in} > 1/R_{rt}$. In the oscillation build-up process all modes (harmonics) are initially excited. But at saturation only modes with gain higher than the threshold are filtered in, and have a chance to survive the oscillation build-up process (Fig.10a).

The steady state output is as in the superradiant emission case (Fig.5) a finite coherent sum of longitudinal modes that lie within the gain bandwidth π/t_{sl} of the FEL. This finite sum of harmonic frequencies looks in the time domain as a periodic train of radiation pulses synchronous and with good overlap with the macropulses of e-beam bunches train that provides the gain. This is an exact analogue of an actively locked conventional *"mode locked laser"*. Also in this case, if the RF frequency is stable over the macropulse, the coherence of the harmonics is very high (if they are filtered out), and is determined by the duration of the macropulse $\Delta\omega \sim 2\pi/T_p$. Namely, the consecutive radiation wavepackets are coherent with each other throughout the macropulse (assuming a single bunch per round-trip).

It is worth noting that high coherence between the radiation wavepackets emitted by consecutive microbunches was measured in a long-wavelength FEL oscillator [19]. This was measured both for the spontaneous and stimulated emission of the FEL. It is remarkable that this coherence was observed when there are several microbunches in the resonator at the same time (RF bunching period shorter than the cavity round-trip time). This is explained there as the result of high
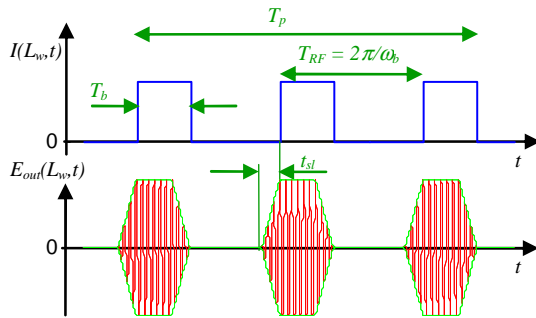

Fig.9: The time domain waveform of the radiation wavepackets emitted at saturation by an RF-Linac FEL oscillator during the electron beam macropulse.
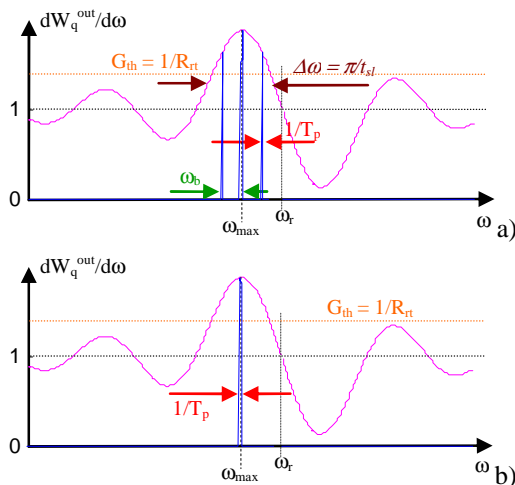

Fig.10: The spectral power and modes structure of saturated FEL oscillator – a)multiple modes, coherently mode-locked in an RF-Linac FEL, b) Single mode operation in a quasi-CW or long pulse (electrostatic accelerator) FEL.

stability of the e-beam RF frequency and the microbunches envelop shapes. It is argued that in the parameters regime of the FELIX FEL [19], the microbunch formfactor (16) is appreciable of the emission frequency, and the superradiant (coherent) undulaotr radiation related to the stable shape of the micropulse current waveform dominates the random shot noise radiation, and consequently determines the phase of all wavepackets. This happened both under conditions of saturated stimulated emission (oscillator lasing) and absence of stimulated emission (no overlap of the recirculating wavepackets).
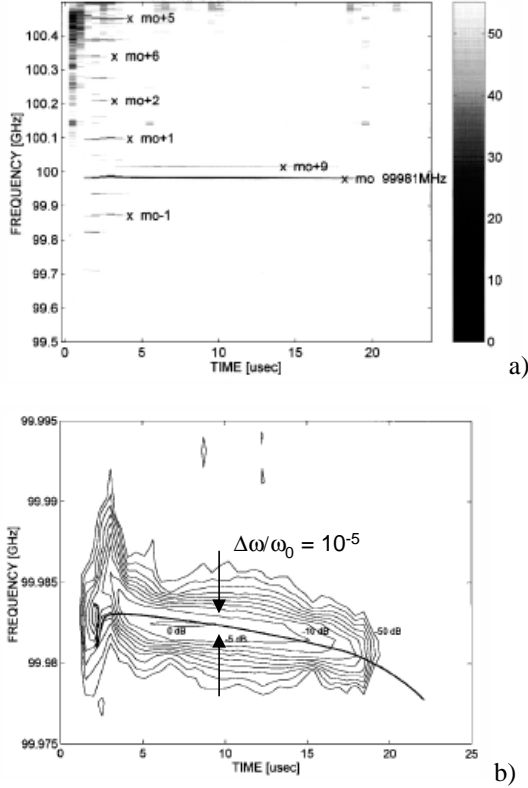

a)

b)

Fig.11: Spectrogram of the radiation output from an electrostatic accelerator FEL oscillator [9].

  a) Multimode spectrum evolving into single mode operation during the oscillation build-up periods.

  b) Fourier transform limited spectrum of the surviving single mode.

Table 1: Intrinsic Linewidth Conditions		
Maser	$\Delta\nu_{maser} = 2\pi kT \dfrac{\left(\Delta\nu_{sp}\right)^2}{P_{gen}}$	Gordon, Zeiger, Townes [11]
Laser	$\Delta\nu_{laser} = 2\pi h\nu \dfrac{\left(\Delta\nu_{1/2}\right)^2}{P_{gen}}$	Schawlow, Townes [12]
FEL	$\Delta\nu_{FEL} = \dfrac{\left(\Delta\nu_{1/2}\right)^2}{I_0/e}$	Gover, Amir, Elias [13]

CW (ELECTROSTATIC ACCELERATOR) FEL OSCILLATOR

What would happen in a CW or a long pulse FEL oscillator (like an electrostatic accelerator FEL)? In this case, there are longitudinal modes due to the round-trip periodicity, but there is no active mode locking. In principle, many longitudinal modes can co-exist within the gain bandwidth, and there is no external que that can phase-lock them.

The oscillation build-up stage involves in this case a mode competition process, which arises when the oscillator approaches saturation and arrives to the non-linear regime. In the FEL, as in other "homogenously broadened lasers", this process ends with single mode operation (see Fig.10b). The single mode laser radiation linewidth is very narrow corresponding to the pulse duration. It is given by the Fourier transform limit $\Delta\omega_{line} \sim 2\pi/T_p$, and it tends to zero as $T_p \to \infty$ (CW operation). An experimental confirmation for the mode competition process and the Fourier transform limited linewidth of the single-surviving mode in an Electrostatic Accelerator FEL was provided in the Israeli FEL [9] (see Fig.11). In [9] a relative linewidth $\Delta\omega_{line}/\omega_0 = 10^{-6}$ was measured at frequency $f_0 = 100$ GHz corresponding to a pulse duration $T_p \sim 10$ μs.

What determines the linewidth in the limit $T_p \to \infty$? This fundamental problem was addressed already in the early days of conventional masers [11] and lasers [12]. In principle the oscillator line breadth is determined by a process of admixture of incoherent radiation with the coherent stored radiation field in the cavity. This process leads to random phase drift of the radiation mode amplitude C_q at the saturation stage (the amplitude is locked by the saturation process). In a maser the intrinsic linewidth results in from incoherent black body radiation emission into the cavity [11]. In a conventional laser, the limiting factor is the quantum spontaneous emission [12]. In the FEL the limiting factor is the spontaneous undulator radiation emission (or the electron beam shot noise) [9, 13]. The three intrinsic linewidth expressions are listed in Table 1.

HIGH GAIN FEL AMPLIFIER

Our analysis of the FEL in the linear regime is based on the Pierce TWT model for TWT [14, 6]. It is found that the amplitude of the radiation mode $C_q(L)$ in an FEL amplifier of interaction length L, depends on the input field amplitude $C_q(0)$ (regular FEL), but also on the amplitudes of the e-beam velocity and current (density) pre-modulation [15, 16]:

$$C_q(L,\omega) = H^E(\omega)\,C_q(\omega,0) + H^\nu(\omega)\,\nu(\omega,0) + H^I(\omega)\,I(\omega,0)$$

(17)

where the transfer functions are:

$$H^E(\omega) = \sum_{j=1}^{3} \text{Res}\left(\frac{(\delta k_j - i\theta)^2 + \theta_{pr}^2}{\Delta}\right) e^{i(k_{zq} + \delta k_j)L} \quad (18.1)$$

$$H^v(\omega) = \sum_{j=1}^{3} \text{Res}\left(\frac{ik_z L / v_{0z}}{\Delta} \cdot P_b^{1/2}\right) e^{i(k_{zq} + \delta k_j)L} \quad (18.2)$$

$$H^I(\omega) = \sum_{j=1}^{3} \text{Res}\left(\frac{(\delta k - i\theta)}{\Delta} \cdot P_b^{1/2} / I_b\right) e^{i(k_{zq} + \delta k_j)L} \quad (18.3)$$

$$P_b = \frac{I_b^2 \sqrt{\frac{\mu_0}{\varepsilon_0}}}{32} \cdot \left(\frac{a_w}{\gamma \beta_z}\right)^2 \cdot \frac{L^2}{A_{em}} \quad (18.4)$$

$$\Delta = \delta k (\delta k - \theta - \theta_{pr})(\delta k - \theta + \theta_{pr}) + \Gamma^3 \quad (18.5)$$

In these formulas we use the "conventional" parameters: θ - detuning parameter; Γ – gain parameter; θ_{pr} – space-charge parameter with reduction factor; L – interaction length; I_b – electron beam current, A_{em} – effective mode area. Here $\delta k = k_z - k_{zq}$ is the modification to the wavenumber of mode q (at fixed frequency ω) due to the interaction. Solution of the Pierce cubic dispersion equation 18.5 and substitution into (17, 18.1-18.3) results in the output radiation field amplitude for all gain regimes and any initial conditions.

In the high gain tenuous beam regime ($\Gamma^3 >> \theta, \theta_{pr}, 1$) one gets for an FEL amplifier:

$$P_q(L, \omega) = \left|\tilde{H}^{FEL}\right|^2 \cdot \left|\check{C}_q(0, \omega)\right|^2 = \left|\tilde{H}^{FEL}\right|^2 P_q(0, \omega) \quad (19.1)$$

for a current (density) pre-bunched FEL:

$$P^{pb-I}(L, \omega) = \left|\tilde{H}^{FEL}\right|^2 \cdot P_b\left(\frac{1}{I_b \Gamma L}\right)^2 \left|\tilde{I}(0, \omega)\right|^2 \quad (19.2)$$

for a velocity pre-bunched FEL:

$$P^{pb-v}(L, \omega) = \left|\tilde{H}^{FEL}\right|^2 \cdot P_b\left(\frac{k_z L}{v_{0z}(\Gamma L)^2}\right)^2 \left|\tilde{v}_z(0, \omega)\right|^2 \quad (19.3)$$

Here

$$\left|\tilde{H}^{FEL}\right|^2 = \frac{1}{9} e^{\sqrt{3}\Gamma L} \cdot e^{-(\omega - \omega_0)^2 / (\Delta\omega_{HG})^2} \quad (19.4)$$

is the power transfer function of the high gain FEL, and

$$\Delta\omega_{HG} = \frac{3^{3/4}}{2\pi} \lambda_w \sqrt{\frac{\Gamma}{L}} \omega_0 \quad (19.5)$$

is the full width of 1/e of maximum of the high gain FEL gain curve and

SASE FEL

The current and velocity modulation amplitudes in (19.2, 19.3) may be deterministic (prebunching) or random (noise). The video presentation in the transparencies demonstrates the meaning and significance of the current and velocity coherent modulation and noise processes.

The SASE FEL is based on amplification of electron beam noise in the FEL high gain regime. To analyze this case it is proper to calculate spectral energy and spectral power parameters instead of the single frequency gain and radiative power parameters (19.1-19.3):

$$\frac{dW_q}{d\omega} = \frac{2}{\pi} \left\langle \left|\check{C}_q(\omega)\right|^2\right\rangle \quad (20.1)$$

$$\frac{dP_q}{d\omega} = \frac{1}{T} \left\langle \frac{dW_q}{d\omega}\right\rangle \quad (20.2)$$

where the averaging is over the electrons random entrance times and T is an averaging time duration longer than the slippage time t_{sl}.

The SASE FEL is nothing but a single path high gain FEL with an effective beam-prebuncing input signal due to current shot noise and velocity shot noise. Near the synchronism frequency its spectral power is a sum of the amplified current and velocity shot noise sources:

$$\frac{dP_q^I}{d\omega} = \frac{2}{\pi} H^{FEL} \cdot P_b\left(\frac{1}{I_b \Gamma L}\right)^2 \frac{\left\langle \left|\tilde{I}(0, \omega)\right|^2\right\rangle}{T} \quad (21.1)$$

$$\frac{dP_q^v}{d\omega} = \frac{2}{\pi} H^{FEL} \cdot P_b \left(\frac{k_z L}{v_{0z}(\Gamma L)^2} \right)^2 \frac{\left\langle |\breve{v}_z(0,\omega)|^2 \right\rangle}{T}$$

(21.2)

where

$$\frac{\left\langle |\breve{I}(0,\omega)|^2 \right\rangle}{T} = e I_b$$

(22.1)

$$\frac{\left\langle |\breve{v}_z(0,\omega)|^2 \right\rangle}{T} = \frac{e}{I_b} |\delta v_z|^2$$

(22.2)

Here δv_z is the axial velocity spread of the electron beam.

Usually the current shot noise is considered the main source for SASE input power and the velocity noise is neglected. This is not self evident. For this assumption to be valid (21.1) should exceed (21.2). Considering (22.1, 22.2) this leads to the condition

$$\frac{\delta v_z}{v_{oz}} < \frac{\Gamma}{k_z}$$

(23)

SPIKING IN SASE-FEL AND THE IMPULSE RESPONSE FUNCTION

Since the SASE-FEL is a wide band amplifier of a wide band incoherent signal (the shot noise), it is no wonder that the spectrum of its radiation output is relatively wide and its temporal waveform is characterized by a random sharp structure (spiky). Fig.12 [10, 17] displays the typical spectrum of a single SASE radiation pulse (Fig.12a), the averaged spectrum over many pulses (Fig.12b) and the spiky time-domain waveform of a single radiation pulse (Fig.12c). One should note that the

relatively high bandwidth of the averaged radiation spectrum ($1/T_{coh}$) is related to the characteristic duration of the spikes (T_{coh}). It is also noteworthy, that the single pulse spectrum contains spectral lines that are very narrow ($1/T_b$) – corresponding to the duration of the e-beam micro bunch - but appear at random centre frequencies.

Since the shot noise spectrum is uniform, the average spectrum of the SASE is determined merely by the transfer functions (18.2, 18.3). Consider now only the current shot noise. It is useful to expand the logarithm of the exponentially growing term in (18.3) (including the phase, namely the imaginary part) to second order in terms of frequency ω around the *synchronism* frequency ω_0. In the high gain (tenuous beam limit) this results in:

$$\tilde{H}^I(z,\omega) \cong \frac{P_b}{3 I_b \Gamma z} e^{-i\pi/12} e^{(\sqrt{3}+i)\Gamma z/2} \times$$
$$\times e^{-(1+i/\sqrt{3})(\omega-\omega_0)^2/2(\Delta\omega_{HG})^2} e^{ikz}$$

(24)

where $\Delta\omega_{HG}$ is the width of the high gain FEL gain curve. Indeed this spectral width is the linewidth $\Delta\omega_{HG} \sim 1/T_{coh}$ of the SASE average spectrum shown in Fig.12b.

It is instructive now to calculate the "impulse response function" corresponding to the complex transfer function (24). This is straightforwardly found by applying an inverse Fourier transformation on (24):

$$E(z,t) = \mathrm{Re}\left\{ \left(P_b \Delta\omega_{HG} / 3^{3/4} \sqrt{2\pi(i+\sqrt{3})} I_b \Gamma z \right) \cdot \right.$$
$$\exp\left[-i\pi/12 + (\sqrt{3}+i)\Gamma z/2 \right] \cdot$$
$$\exp\left[+i\left(\omega_0\left(t - \tfrac{z}{c} - t_0\right) - (\Delta\omega_{HG})^2\left(t - \tfrac{z}{c} - t_0\right)^2 / 8 \right) \right] \cdot$$
$$\left. \exp\left[-(\Delta\omega_{HG})^2\left(t - \tfrac{z}{c} - t_0\right)^2 / 8 \right] \right\}$$

(25)

This function is displayed in Fig.13. It depicts (within the quadratic expansion approximation a Gaussian wave form envelope of width $T_{coh} \sim 1/\Delta\omega_{HG}$. It also reveals an
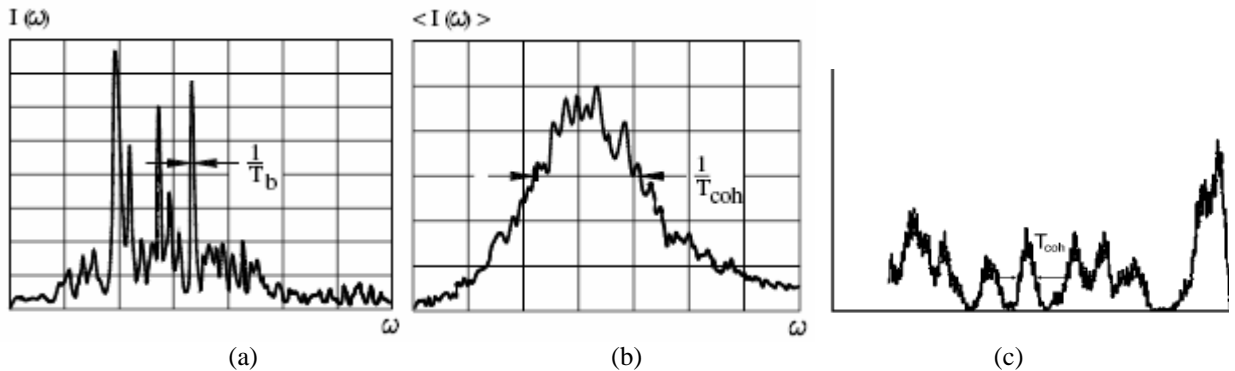

Fig.12: Simulation data of SASE radiative emission [9, 16]:
  a) Single pulse spectral power,   b) Spectral power averaged over many pulses, c) Time domain "Spiky" intensity distribution of a single pulse.

inherent (negative) chirp of the centre frequency

$$\frac{d\omega}{dt} = \frac{d^2\varphi}{dt^2} = -(\Delta\omega_{HG}/2)^2 \qquad (26)$$

The impulse response function (25) is the coherent field wave-form created by an impulse of charge (of duration much shorter than the radiation wavelength), which is
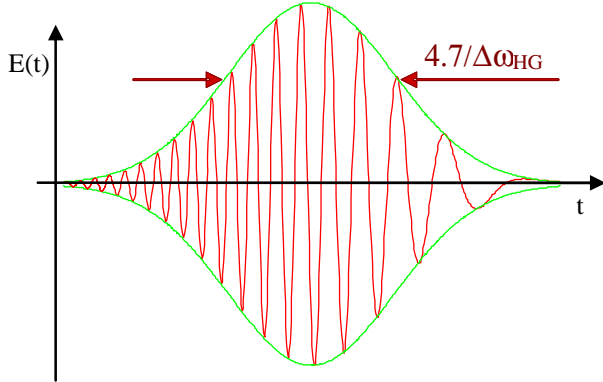

Fig.13: The time domain charge-impulse response function of an FEL in the high gain regime (Eq. 20).
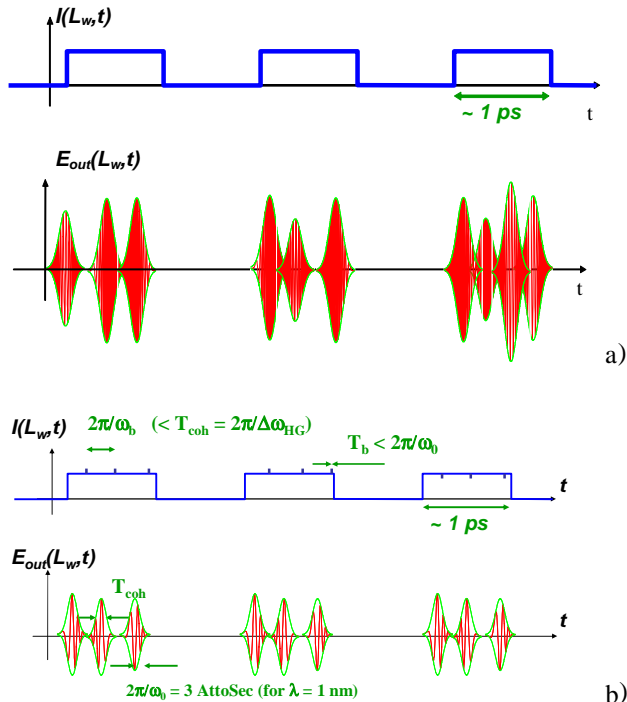

Fig.14: Spikes emission in SASE FEL within the micropulses duration: a) Random emission
b) Phase-locked coherent spikes emission initiated by subharmonic current prebunching.
Prebunching can be produced by a train of superimposed positive or negative current impulses or any stable periodic current waveform of high harmonic contents.

superimposed at entrance over a uniform e-beam current I_b. it is quite natural to identify it with the spikes phenomenon shown in Fig.12c. The physical picture of the phenomenon is based on appearance of random electron bunches (current fluctuation) on the electron beam current entering the interaction region. This current is uniform on the average, but fluctuates because of the randomness of electrons generation in the cathode ("shot noise"). The random electron bunches start radiating *superradiantly* right at start, and their radiation wavepackets dominate over the spontaneous radiative emission from the other uniformly (but randomly) injected electrons. Due to the forward slippage effect of the radiation wavepacket and the high gain stimulated emission process, the random electrons, that are flowing within a cooperation length $v_z T_{coh}$ ahead of the initial radiating random bunch, are induced to emit at the same frequency and phase (except for the inevitable chirp effect), and consequently a coherent wavepacket (Fig.13) is emitted. The output wavepacket duration $T_{coh} = \pi/\Delta\omega_{HG}$ (determined by the high gain FEL bandwidth 19.4) is the minimal width of the spike. Spikes that are excited by random bunches in time always shorter than T_{coh} merge into one spike. Assuming there are always enough random bunches to negate presence of long "silent" spaces between the spikes; one can estimate that the average number of spikes in a bunch of duration T_b is T_b/T_{coh} [10]. Fig.14a displays the spikes waveforms of this physical model. It should be compared to the simulation spiky pattern of Fig.12c. If $T_b \cong T_{coh}$ then there is only one spike in the macropulse duration [17]. In this case the SASE radiation is as coherent as can be (Fourier transform limited). Its spectral width is $\cong \pi/T_{coh} = \pi/T_b$. It can be narrowed down only if pulse stretching techniques can be employed.

CONDITIONS FOR COHERENT X-UV FEL

It is well known that the radiation output of SASE FEL is spatially coherent (due to the optical guiding effect). This is the reason why SASE FELs can be so much brighter than any other existing radiation source in this spectral regime. However there will be even greater interest in this source if it would be also temporally coherent and stable (pulse to pulse). How can a SASE FEL be turned into a coherent radiation source?
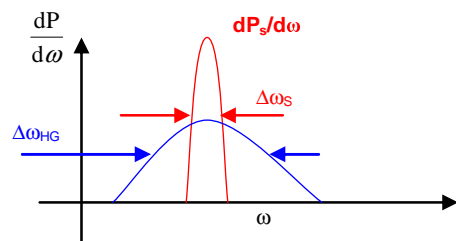

Fig.15: Spectral power of the coherent radiation output of the FEL amplifier (red) and the SASE (shot noise) radiation (blue).

Realizing that the SASE-FEL is an amplifier of noise, it is evident that what is required is a coherent input signal. The input signal can be a coherent radiation wave (this is sometimes called seed radiation injection), and there has been intensive studies of developing an appropriate coherent seed radiation sources based on high harmonic multiplication of intense laser pulses in gas. Another scheme is based on filtering the undulator synchrotron radiation after a few sections of the undulator, and reinjecting the narrower bandwidth radiation into the undulator for high gain amplification.

Another approach for attaining coherent emission from SASE-FEL is based on coherent prebunching of the electron beam (within the duration of its pSec microbunches) at the radiative emission frequency of a high power optical laser or its subharmonics. This process can be repeated in several steps, in which the bunched radiation is amplified at high gain, and then high harmonics of the electron bunching are filtered out and amplified again, and so on (High Gain High Harmonic Generation – HGHG [21]).

In all of these schemes the condition for attaining coherent high power output radiation is that the coherent input signal will be significantly larger than the noise. In the first case of *seed radiation injection* (coherent amplification) a simple criterion can be inferred by comparing (19.2) to (21.1-22.2). Assuming the current shot noise is dominant, this condition is:

$$P_s(0) >> P_b \frac{e}{I_b (\Gamma L)^2} \Delta\omega \qquad (27.1)$$

Here $\Delta\omega$ is the frequency bandwidth of the detection system in which inevitable (now undesirable) SASE radiation is collected. If there are no means of filtering available, then $\Delta\omega = \Delta\omega_{HG}$ - the SASE radiation bandwidth. In any case $\Delta\omega_s$, $\pi/T_b < \Delta\omega < \Delta\omega_{HG}$, where $\Delta\omega_s$ is the linewidth of the injected input radiation and π/T_b is the Fourier limited bandwidth of the finite pulse. Similar condition can be derived for the required prebunching current required to dominate the current shot-noise by comparing (19.2) to (21.1, 22.1):

$$\left| \tilde{I}(0,\omega) \right|^2 >> \frac{2}{\pi} e I_b \Delta\omega \qquad (27.2)$$

PHASE LOCKING THE SPIKES

If sufficient coherent seed radiation input power is attainable it makes the output power of the FEL amplifier coherent as well. But other aspects of the *seed radiation injection* approach, as tunability and operating wavelengths range still need to be addressed. The *current prebunching* approach may provide more options of frequency tunability and short wavelengths availability.

But its realization requires more intricate conceptual schemes.

Much insight into this problem may be gained from the physical description of the radiation processes in the previous section. In particular it is worth noting the striking correspondence between the emission of single mode undulator radiation wavepackets by a single electron (or single bunch) (10) (in the frequency domain) and (11) (in the time domain) and the corresponding expressions of spectral transfer function (24) and impulse response function (25) in the case of FEL in the high gain regime. In the first case the wavepackets emission process is spontaneous (or superradiant in the case of a bunch) and no supporting medium is required for the wavepacket emission. In this case Eq.11 (Fig.4) is the explicit time-domain expression of the wavepacket emitted in the undulator from a particulate charge of *one electron* (e). In the second case, (Eq.25) (Fig.13) is the radiation wavepacket emitted by a *current impulse of a unit charge,* and the excitation of this wavepacket is conditioned on the presence of an electron beam medium (assumed uniform) in front of the beam current impulse. Its emission process involves stimulated emission and bunching of the e-beam, in contrast to the first case.

In both cases the coherence of the total radiation of the e-beam depends on the phase relation between the emitted respective wavepackets by the charged particles or by the bunches. In the first case, when the electrons enter into the undulator at random, the superposition of the radiation wavepackets (11) in (5) produces incoherent radiation (or more correctly - partially coherent radiation with coherence time t_{sl}). Analogously, in the SASE case, the superposition of the impulse response waveforms (23) from random bunches (the "spikes") produces partially coherent radiation of coherence length $T_{coh} \sim 1/\Delta\omega_{HG}$.

How can we turn the SASE radiation to be coherent? In analogy to the case of superradiant emission from a periodic train of bunches it is suggested that periodic superposition of current impulses on top the uniform current of the microbunch will phase-lock the spikes into a coherent train of wavepackets with distinct phase relation of the "carrier" radiation waves along the entire microbunch (see Fig.14b as opposed to Fig.14a). This situation is analogous to the one described by Fig.5.

How to create the sub optical period current impulses is still an open challenge. It is important to note that the current perturbation does not have to be positive (see third pulse in Fig.15b). It can be of any shape, as long as it is kept periodic along the pulse with accuracy (stability) better than one optical period (which may be AttoSeconds in the X-UV regime!), and as long as it is "sharp" enough to produce significant current amplitude of Fourier harmonics to satisfy (27.2).

It is noteworthy that the prebunching frequency does not need to be equal to the radiation emission frequency and it can be a high sub-harmonic of this frequency. In this case the coherent spectrum may contain several harmonics as in Fig.5c, however as discussed in that context, each harmonic would be coherent throughout the

entire duration of the pulse, and its linewidth is Fourier transform limited ($2\pi/T_p$). In principle the harmonics can be filtered out by physical means or by numerical processing of the data acquired by a coherent detection system data in a spectroscopic application.

Note that if single harmonic operation is desired it is not necessary that the prebunching frequency be equal to the radiation frequency. It is only required that the bunching frequency ω_b (sub-harmonic n_H of the radiation frequency ω_0) will be larger than the FEL high gain bandwidth (compare to (15)):

$$\omega_b = \frac{\omega_0}{n_H} > \Delta\omega_{HG} = \frac{3^{3/4}}{2\pi}\lambda_w\sqrt{\frac{\Gamma}{L}}\,\omega_0 \qquad (28)$$

$$\text{or } n_H \langle \frac{2\pi}{3^{3/4}}\sqrt{\frac{\Gamma}{L}}\Big/\lambda_w$$

The spectrum will look then as in Fig.5b, but with a single harmonic frequency of linewidth $2\pi/T_p$ under the amplifier gain curve. In time domain the radiation waveform will look then as in Fig.14, without spacing between the overlapping phase locked spikes. In the extreme limit of (25) the waveform would be a single coherent wavepacket along the entire pulse (microbunch) duration T_p.

As mentioned above, realization of the high harmonic bunching schemes is still a challenge. We examine in principle (Fig.16) a scheme of optical laser bunching, employed on a uniform electron beam, which is trapped by the ponderomotive wave of a wiggler and an external coherent bunching laser. Fig.16a displays the θ-ψ phase-space electron distribution of one pondermotive period exactly after one quarter period of synchrotron oscillation [16]. The current distribution along one bunching period is shown in Fig.16b and its Fourier harmonic amplitudes are shown in Fig.16c. Notice that significant amplitudes can be attained even at very high harmonics. However, in practice realizing the sharp current waveform structure of Fig.16b may be difficult, because of the electron beam energy spread and finite emittance. One should also bear in mind that in this scheme also velocity (energy) modulation of the beam is generated collaterally, and this contribution of to the radiation power (18.2) should be taken into account, including the consideration of the relative phase between the velocity and the current modulation.

A third scheme that should be considered for phase locking and increasing the coherence of the radiation in a SASE FEL consists of imposing periodic perturbation on the wiggler (e.g. periodic dispersive sections) [20]. The filtering effect of the periodic structure may be viewed as the analogue of linewidth narrowing of radiation emitted in a Fabri-Perot resonator. It is speculated (but needs further study) that if the SASE FEL in such a structure arrives to saturation within the wiggler length, nonlinear process of mode competition between the filtered spikes will lead to further increase of coherence and stability in
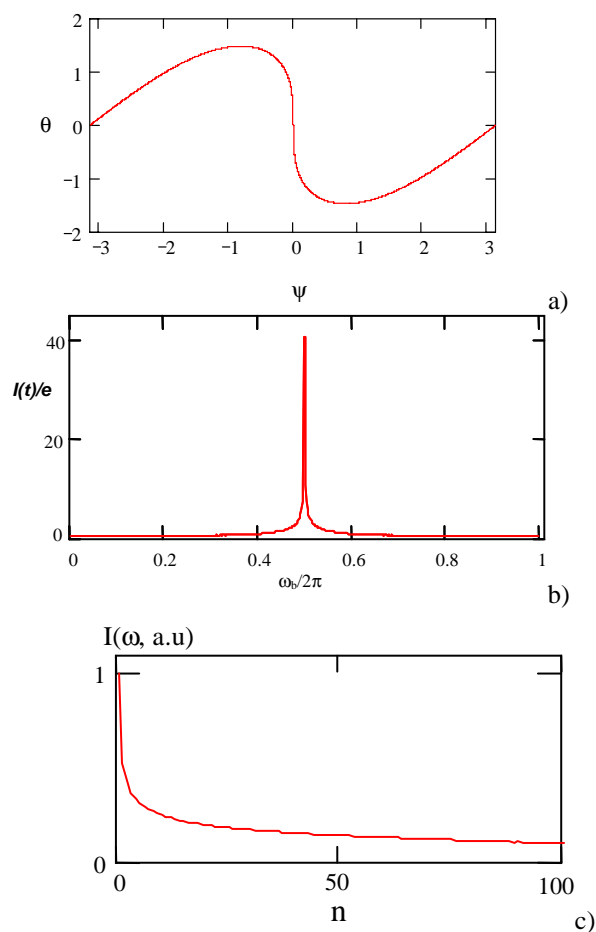

Fig.16: Bunching of a cold beam by the pondermotive wave (pendulum equation model [15]):
a) Electron detuning phase distribution in one period after one quarter period of synchrotron oscillation
b) Corresponding current waveform in one bunching period
c) Fourier harmonic amplitude of the waveform in (b).

analogy to the CW FEL oscillator case discussed previous.

REFERENCE

1. A. Gover, PRL, <u>96</u>, 124801 (2006); A. Gover, Phys.Rev ST-AB, <u>9</u>, 060703, (2006).
2. A.A. Barybin, "*Modern electrodynamics and coupled-mode theory: application to guided-wave optics*", Rinton Press, (2002).
3. A. Gover, Phys.Rev. ST–AB, <u>8</u>, 030701 (2005).
4. R.H. Dicke, Phys.Rev., <u>93</u>, 99 (1954).
5. G.L. Carr et al, Nature, <u>420</u>, 153 (2002).
6. A.Gover, P. Sprangle, QE-<u>17</u>, 1196 (1981).
7. A. Gover et al, Phys.Rev.Lett., <u>72</u> 1192 (1994).

8. S.E. Korbly et al, PRL, 94, 054803/1 (2005).

9. A. Abramovich et al, Phys.Rev.Lett., 82, 5257 (1999).

10. S. Krinski and R.L. Gluckstern, Phys.Rev. ST-AB, 6, 050701, (2003).

11. Gordon, Zeiger, Townes, Phys.Rev., 99, 1264 (1955).

12. Schawlow and Townes Phys.Rev., 112, 1490 (1958).

13. A. Gover A. Amir, L. Elias, Phys.Rev.-A, 35, 164 (1987).

14. J.R. Pierce, "*Traveling-Wave tubes*", Toronto,Van Nostrand, (1950).

15. I. Schnitzer, A. Gover, NIMPR A237, 124 (1985).

16. A. Gover, "Lasers: Free Electron Lasers" *Encyclopedia of Modern Optics*, Ed. R. D. Guenther, D. G. Steel and L. Bayvel, Elsevier, Oxford (2005).

17. R. Bonifacio et al, PRL, 73, 70 (1994).

18. E. L. Saldin, E. A. Schneidmiller, and M.V. Yurkov, *The Physics of Free Electron Lasers,* Chap. 6 (Springer-Verlag, Berlin, 2000).

19. H.H. Weits, D. Oepts, IEEE QE, 35, 15, 1999.

20. Y.C. Huang – private communication.

21. L.H. Yu et al, Phys.Rev.Lett., 91, p 74801/1, 2003.

22. M. Arbel et al, Nucl.Inst.Meth.Phys.Res., A445, 247 (2000).